Penning Trap Experiments at the University of Washington and at NIST in Boulder

F.L. Moore

Time and Frequency Division
NIST
Boulder, Colorado 80303

Abstract

I briefly describe and extensively reference the work accomplished using Penning traps at both the University of Washington and NIST (in Boulder). Among this work are tests of QED, CPT, general relativity, and quantum mechanics. Also mentioned are several measurements of fundamental constants, a laser cooled atomic clock, a frequency divider, and studies of nonneutral plasmas.

INTRODUCTION

I will describe two basic types of Penning trap experiments. In the first class of experiments the interaction of the trapped particle with an extremely harmonic trap is measured and in a sense one is preforming spectroscopy on a "geonium" type atom[1] to get at the physics of interest. In this case the trapped particle is considered only as a charged mass and detection and cooling (usually to 4 K) is accomplished with RF drives and resistive losses. In the second class of experiments the Penning trap is used primarily as a storage device for cold ions. Lasers are used to detect and cool the ions (usually to ≈ 10 mK). One can then either take advantage of the long interrogation times and relatively systematic free environment to do spectroscopy on the ions or study the ions as a nonneutral or one component plasma. An experiment that couples together two traps to extend the lower temperature advantage of laser cooling to a larger class of Penning trap experiments is also mentioned.

Throughout this article we limit our discussion to experiments which were conducted or conceived at the University of Washington or at the National Institute of Standards and Technology in Boulder. This does not reflect upon the scientific merit of the diverse field of experiments done in Penning traps carried out by other groups but is merely due to space limitations. As partial amends for this injustice and to whet the reader's intellectual appetite, I give references to a sampling of some of the experiments done by other groups.[2–6]

BASIC HARMONIC PENNING TRAP

The traditional[1] harmonic Penning trap consists of five cylindrically symmetric electrodes (see Fig. 1) designed to generate the quadratic potential

$$V = V_0 \, \frac{z^2 - \rho^2/2}{2d^2} + V_0 C_4 \, \frac{z^4 - 3z^2\rho^2 + \frac{3}{8}\rho^4}{2d^4} + \cdots \qquad (1)$$

Here V_0 is approximately the potential difference between the ring and end cap electrodes, which have contours that follow hyperboloids of revolution, and d is the characteristic dimension of the trap defined in terms of the ring radius R_0 and half the end cap spacing Z_0. It is defined by

$$d^2 = \frac{Z_0^2 + R_0^2/2}{2}. \qquad (2)$$

The voltage on the guard electrodes is typically adjusted to minimize the value of the fourth-order corrections to this trapping potential (C_4).

The quadratic nature of this potential confines the charged particle axially and induces harmonic motion at an angular frequency given by

$$\omega_z^2 = \frac{eV_0}{md^2}. \qquad (3)$$

Radial confinement is provided by a strong magnetic field **B** applied along the z axis. This induces a cyclotron-like motion at the frequency

$$\omega_c' = \omega_c - \frac{\omega_z^2}{2\omega_c'}, \qquad (4)$$

which is the free-space cyclotron motion at $\omega_c = eB/(mc)$ reduced because of perturbations caused by

[1] Traps made of cylinders[7] are finding wide use because of their increased access in the axial direction. These and other nontraditional[8] designs suffer from a smaller harmonic trapping volume and usually have a smaller coupling to the trapped particle thereby reducing cooling and detection efficiency.

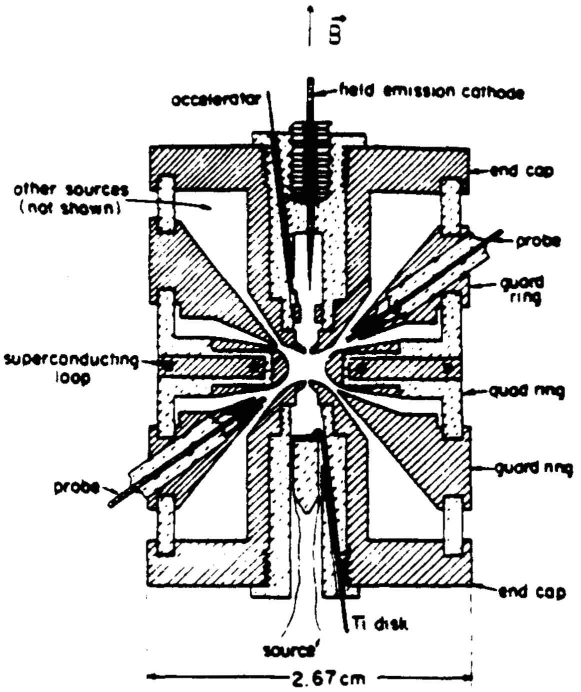

Figure 1: A detailed scale drawing of a harmonic Penning trap. The hyperbolic end caps are at a DC ground and the hyperbolic quad ring is at a potential V_0. This produces a harmonic electrostatic well in the axial direction. The potential on the guard electrodes is adjusted to minimize the fourth-order electrostatic terms of the trap. Radial confinement comes from a 6 T axial magnetic field which is stabilized by a superconducting double loop[9] placed in the ring electrode. Also shown are the field emission cathode, accelerator, and Ti reflection disk which generate a variable energy, multi-pass, ionizing electron beam. The probe electrodes are used to produce the necessary spatial gradient in the sideband cooling drive (from Ref. [26]).

the radial electric fields. This perturbation is the familiar $\mathbf{E} \times \mathbf{B}$ drift velocity which, coupled with the azimuthal symmetry of the trapping fields, generates a slow circular magnetron motion at the frequency

$$\omega_m = \frac{\omega_z^2}{2\omega_c'}. \tag{5}$$

This magnetron motion is unstable because Laplace's equation, coupled with the electrostatic well in the axial direction, implies an electrostatic hill in the radial direction. The damping time, however, is extremely long so for all practical purposes the motion is stable.

In principle the free-space cyclotron frequency can be obtained from Eq. (4) and Eq. (5) by measuring ω_c' and one of the other two normal-mode frequencies. In practice it is more prudent to measure all three normal mode frequencies and derive the free space cyclotron frequency by using the quadrature equation

$$\omega_c^2 = (\omega_c')^2 + \omega_z^2 + \omega_m^2, \tag{6}$$

which can be obtained by squaring Eq. (4). Equation (6) has been shown[10] to be invariant under all quadratic field perturbations such as cross terms due to an elliptical electric field geometry in addition to a misalignment between the magnetic field and the trap's electric axis.

The first class of experiments is fundamentally tied to the ability to measure this cyclotron frequency.

g-2 EXPERIMENT

A fair fraction of the current work done in ion traps has its roots in the early g-2 experiments. For instance laser cooling,[11] fundamental to many studies of ions in both Penning, Paul,[12] and neutral traps,[13] is an extension of sideband cooling[11,14] developed to reduce the magnetron motion. The field of mass spectroscopy using a harmonic Penning trap began in the preliminary g-2 experiments with the comparison of the mass of the positron to that of the electron[15] which, incidentally, represented the first long term confinement of low energy antimatter. Therefore, in describing the basic g-2 experiment, I will develop most of the framework necessary for the other experiments discussed in this paper. I will not go into extensive details about this or any other experiment; instead I direct the reader to the original publications. For the g-2 experiment there are three excellent review articles[16–18].

In the g-2 experiment the only electron motion that is detected directly is the axial oscillation. This motion induces oscillating currents of $\approx 10^{-14}$amp in the end caps of the trap. The capacitance of one end cap, together with a helical resonator, form a tuned circuit. On resonance this tuned circuit's impedance is purely resistive and damps the axial motion to the ambient temperature of the 4 K liquid helium bath. These currents, and therefore the axial motion, are monitored with the cryogenic super-heterodyne detector shown in Fig. 2(a). The phase relation between the rf drive and the resulting driven harmonic axial motion can be recorded as the drive is swept through resonance, as shown in Fig. 2(b), or it can be used as an error signal in a lock loop that feeds a correction voltage back to the ring electrode to frequency lock the axial motion to the drive synthesizer. Perturbations introduced to shift the axial frequency will then produce a corresponding shift in the correction voltage which can be continuously monitored.

For the existing g-2 measurement this perturbation, called the "magnetic bottle," is the potential energy associated with the interaction of the trap-

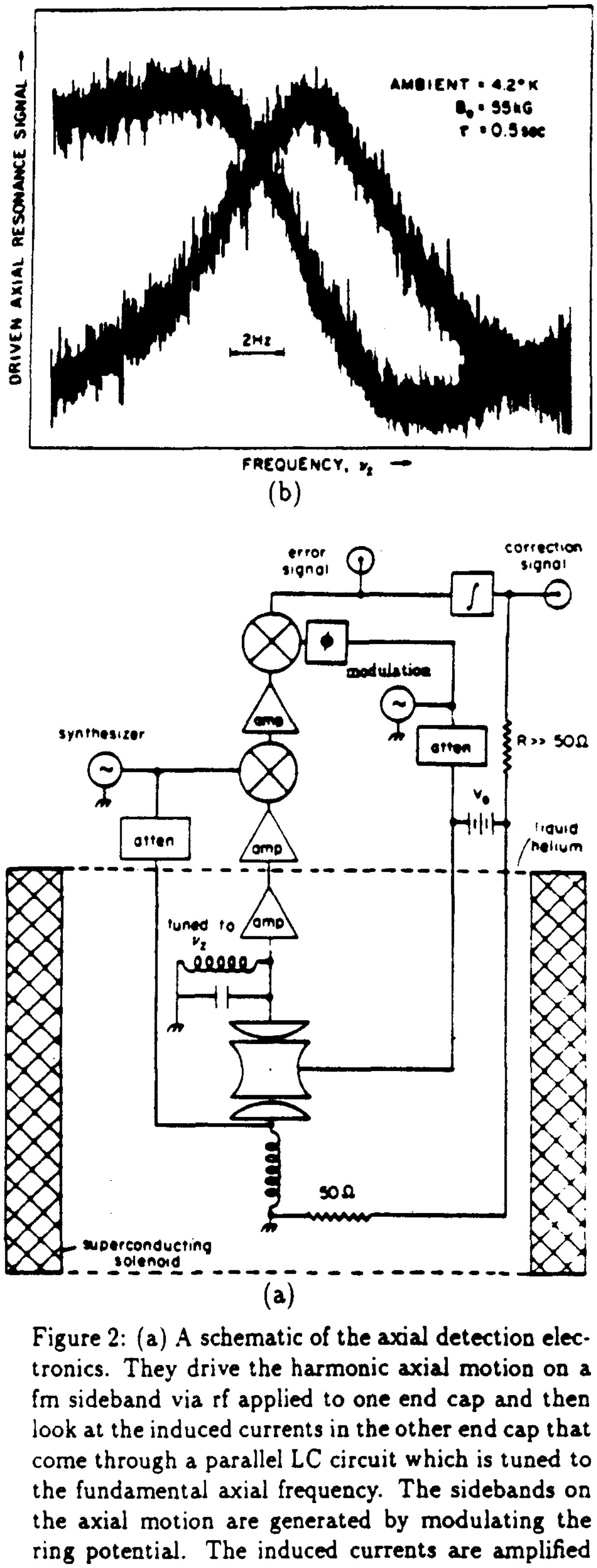

Figure 2: (a) A schematic of the axial detection electronics. They drive the harmonic axial motion on a fm sideband via rf applied to one end cap and then look at the induced currents in the other end cap that come through a parallel LC circuit which is tuned to the fundamental axial frequency. The sidebands on the axial motion are generated by modulating the ring potential. The induced currents are amplified by a GaAs FET submersed in liquid helium and then mixed to DC to display the phase relation between the drive and the driven axial motion. This phase relation, shown in (b) (from Ref. [14]), is used as an error signal that is integrated and added to the ring as a correction voltage to frequency lock the axial resonance to the stable drive.

ped electron's magnetic dipole moment μ with a quadratic axial gradient in the magnetic field. This μz^2 dependent potential adds to the original axial well depth. The monitored axial frequency then becomes a function of the magnetic moment of the trapped particle. By sweeping a microwave drive through resonance, the cyclotron motion is excited out of its ground state[2] thereby increasing μ and inducing a shift in the correction voltage to counteract the μz^2 induced shift in the axial frequency. Similarly if the spin of the electron is flipped the corresponding change in μ can also be observed in the axial correction voltage. This basic detection scheme has been referred to as the "continuous Stern-Gerlach effect."[19]

A subtlety of this experiment is that a simultaneous cyclotron and spin-flip transition is driven by an anomaly drive at the difference between the cyclotron and the spin precession frequency. This measures the anomaly in the g value directly and improves the measurement of the g value by approximately three orders of magnitude. The magnetic field is calibrated by normalizing the anomaly resonant frequency to the cyclotron frequency and perturbations due to the trap's electric field are eliminated by analyzing the data in the co-moving magnetron frame.

The current measurement[20] of the electron's g-value is in good agreement with QED calculations. This check of QED is limited by the uncertainty in the condensed-matter measurements of α [21]. In fact the most precise measurement of α is obtained by assuming QED to be a valid theory and calculating α_{QED}[16] from the measured g value. This experiment has also been performed on positrons and a comparison of the g-values[20] of this matter/antimatter pair is the most stringent test of CPT invariance for Leptons. A comparison of the positron and electron cyclotron frequency compares their respective charge to mass ratio[15] and in that sense is also a check of CPT.

The dominant width and asymmetries in the cyclotron and anomaly resonances are due to thermal axial motion in the "magnetic bottle." There have been three basic approaches proposed to reduce these asymmetrical widths: (a) detection of the magnetic resonances through relativistic effects[22] thereby eliminating the need for a bottle; (b) modulating the bottle,[9] thereby symmetrizing the resonance and, through the marvels of phase sensitive detection, reducing the size of the bottle; and (c) cooling the

[2]The cyclotron motion is in thermal equilibrium with the 4 K trap via radiative processes. In a magnetic field of [illegible] T [illegible] spends most of the time in the ground state.

electron to a zero point axial energy and detecting quantum excitations, both by coupling to a laser cooled ion in an independent trap.[23] To date none of these new schemes has been competitive with the method described above.

MASS SPECTROSCOPY

To the extent that B_0 is constant and charge is quantized, mass ratios can be determined by cyclotron frequency ratios. Use of Eq. (6) to determine the free space cyclotron frequency eliminates all the perturbations due to the quadratic electric fields of the trap. As described earlier, the guard voltage is adjusted to eliminate the fourth-order electric fields. If sideband cooling is then used to confine the trapped particle to a small volume, this measure of the free space cyclotron frequency becomes relatively systematic free.

The first use of the harmonic Penning trap as a mass spectrometer was in the above mentioned comparison of the mass of the positron to that of the electron as a check of CPT. Another was the measurement of the proton/electron mass ratio,[24] which is a key parameter in the least-squares adjustments of the fundamental constants. In this experiment the electron's cyclotron frequency was measured by methods identical to the g-2 experiment. The proton's axial motion was also detected as described in the g-2 experiment; however, the magnetic dipole moment associated with the proton's motion scales with its inverse mass and is therefore to small to be coupled into the axial degree of freedom with any reasonably sized "magnetic bottle." Since the proton's cyclotron motion is only 80 MHz at 6 T, direct detection of this motion can be accomplished if the ring is split. Figure 3 shows schematically how this was accomplished. A similar approach has recently been employed to make a "thousandfold improvement" in the mass comparison of the proton to antiproton[25] which is the most stringent test of CPT invariance for baryons.

In building a general purpose mass spectrometer, direct detection of the cyclotron motion by the currents they induce in the trap's electrodes becomes cumbersome because it requires several tuned preamplifiers for each ion species to be studied in the trap. In addition, direct detection of the image currents of the cyclotron motion requires a strong coupling to the preamplifier. This strong coupling necessarily broadens the cyclotron resonance and can therefore reduce cyclotron resolution.

A new technique called anharmonic detection[26] was developed to get around these problems. In this new approach the cyclotron energy is coupled into the axial well depth through the fourth-order electro-

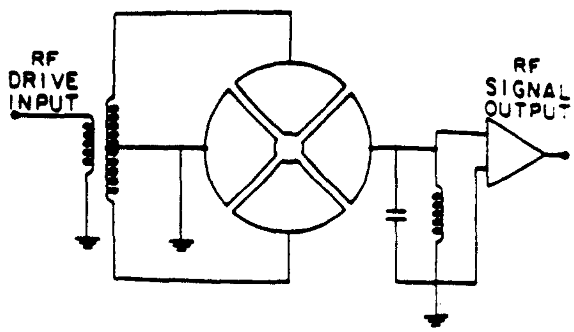

Figure 3: Direct detection of the image currents due to the proton's cyclotron motion was obtained by splitting the ring electrode into four quadrants. A tuned pre-amplifier monitors the currents induced in one ring quadrant. This signal is mixed to DC with a heterodyne system similar to that used for the axial motion. The drive is applied with equal amplitude but 180° out of phase to apposing quadrants orthogonal to that which contained the pre-amplifier. This is done to minimize the drive entering the pre-amplifier directly. This direct drive would otherwise swamp the signal due to the proton's image currents (from Ref. 24).

static term in Eq. (1) (or to be more specific through the $\rho^2 z^2$ term). RF drives are then used to manipulate the cyclotron energy, and corresponding shifts in the feedback voltage of the axial lock are observed. This detection scheme has a one-to-one correspondence to that which used the magnetic bottle; however the electrostatic nature of this perturbation minimizes systematics induced in the cyclotron frequency.

With this new approach a resolution of 0.01 ppb in the cyclotron resonance has already been demonstrated. In addition, its broadband nature allows mass comparisons between any two stable ions in the trap. A host of mass spectroscopy experiments has been performed or proposed in addition to those described above. We list them now, keeping in mind that cyclotron resolution of 0.01 ppb has been demonstrated and that mass comparisons at the 0.01 ppb are therefore conceivable.

The atomic mass of the proton has recently been improved[27] by comparing the cyclotron frequency of a $^{12}C^{+4}$ ion to that of a proton in a Penning trap, and then taking into account the missing mass and binding energy (E_B) of the four electrons:

$$\frac{m_{C^0}}{m_{p^+}} = \frac{m_{C^{4+}}}{m_{p^+}} - \frac{E_B}{m_{p^+}} + 4\frac{m_{e^-}}{m_{p^+}}.$$

The neutron mass can be accessed through the deuterium ion. Consider the following neutron capture:

$$n + p^+ \rightarrow {}^2\mathrm{H}^+ + \gamma.$$

By applying conservation of energy and then normalizing these energies to the proton's mass we get

$$\frac{m_n}{m_{p^+}} = \frac{m_{^2H^+}}{m_{p^+}} + \frac{E_\gamma}{m_{p^+}} - 1. \qquad (9)$$

The neutron/proton mass ratio can therefore be measured by comparing cyclotron frequencies[28] of the deuterium ion to that of the proton and using the existing measured value[29] of $(E_\gamma/m_{p^+} - 1)$.

One method of directly measuring the neutrino mass is through the tritium β-decay experiments in which the emitted electron's energy spectrum is fit to a Kurie plot.[30] This basic two-parameter fit, involving the neutrino mass m_ν and the end-point energy E_0, is usually complicated by atomic/molecular final state corrections and uncertainties in the electron spectrometer resolution function. Possible systematic errors due to these complications can be checked and/or reduced by an independent measurement of the end-point energy which can be determined by a measurement of the mass difference between tritium and He-3. This has also recently been accomplished [31] using cyclotron measurements taken in a harmonic Penning trap.

Finally there are two proposed mass spectroscopy experiments related to tests of QED. The comparison of the measured g-value of the electron to low field QED calculations is limited by the condensed-matter measurement of the fine structure constant α. This measurement of α involves some rather difficult calibrations to several fundamental constants. Greene and Deslattes[32] have suggested a measurement of α that involves mass ratio measurements and is calibrated only by the standard second, thereby getting around these difficult calibrations.

If we consider a neutron capture equation similar to Eq. (8), but involving a generic atom ^{j+1}X, and as before invoke conservation of energy and normalize the result to the proton's mass, we get

$$\frac{m_n}{m_{p^+}} = \frac{\Delta m(^{j+1}X, ^{j}X)}{m_{p^+}} + \frac{E_\gamma}{m_{p^+}}. \qquad (10)$$

The fine structure constant α can then be introduced by using the definition of the Rydberg constant to replace E_γ with its measured wavelength. Algebraically solving for α then gives

$$\alpha^2 = 2R_\infty \left[\frac{m_n}{m_{p^+}} - \frac{\Delta m(^{j+1}X, ^{j}X)}{m_{p^+}}\right] \frac{m_{p^+}}{m_{e^-}} \lambda_\gamma \qquad (11)$$

The Rydberg constant, mass ratios (ratios of cyclotron frequencies), and λ_γ are all calibrated against the standard second, and so would this measure of the fine structure constant. A possible candidate for this experiment is the neutron capture in a ^{14}N atom.

Since most calculations in QED are perturbative, they are more likely to fail in the high field limit than in the low field limit checked by the g-2 experiment. A Lamb shift measurement in a high Z atom would test QED in the strongest **E** field accessible in the lab. The Lamb shift scales as Z^4/n^3 and for hydrogen-like uranium the ground state is about 500 eV, or 2.3 ppb of its 220 GeV rest mass. By comparing the mass difference between the bare nucleus $^{238}U^{92+}$ and hydrogen-like $^{238}U^{91+}$ one can effectively "weigh" the ground state energy[26]. Subtracting the calculated Dirac contribution would then give a measure of the Lamb shift.

ELECTRON DIVIDER

The last experiment which falls into the first class of geonium type experiments involves the nonlinear interaction of a trapped electron's cyclotron motion with a drive at the nth harmonic of ω_c. There are two basic approaches. In one[33] the Doppler shift associated with the oscillatory cyclotron motion at ω_c, effectively frequency modulates the incoming drive field. For all practical purposes the drive is seen to have components at the frequency $\omega_D \pm n\omega_c$. If the drive is at the nth harmonic of the cyclotron frequency ($\omega_D = n\omega_c$), the effective nth lower sideband of this drive will be at ω_c and should therefore excite the cyclotron motion. This driven cyclotron motion will then be phase coherent with the nth subharmonic of the drive. There is hope that n can be made large enough to phase coherently divide optical frequencies down to the microwave region in a single step. Another approach[34] is to tightly focus the drive. Cyclotron motion in and out of this focused drive is then an effective amplitude modulation. This effective modulation can be used in a similar fashion to make a frequency divider.

LASER COOLED ATOMIC CLOCK

In the second class of experiments the Penning trap (see Fig. 4) is used primarily as a storage device where typically large numbers of ions are studied. With extremely long storage times (and therefore interrogation times), ion spectroscopy can be performed with unprecedented resolution, and when laser cooling is available, the low temperatures achieved drastically reduce the velocity dependent systematics that usually limit high resolution spectroscopy.

Along these lines we will describe a "clock" experiment [35] whose high resolution has been used to test several fundamental theories of physics.

In addition to the Doppler perturbations, we must consider perturbations associated with the Penning trap's primary fields. The laser cooled ions seek the

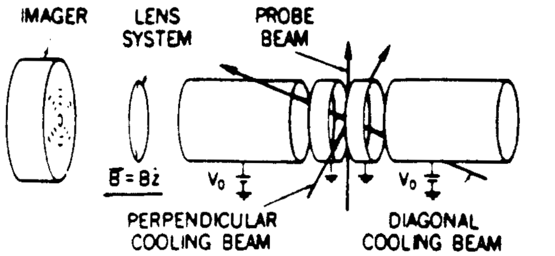

Figure 4: Schematic drawing of the trap electrodes, laser beams, and the imaging system. The overall length of the trap is 10.2 cm. The trap consists of two end cylinders at a typical voltage of 20 V and two electrically connected (and typically grounded) central cylinders. The inner diameter of the trap is 2.5 cm. The ion clouds are typically less than 1 mm in both diameter and axial length. This trap is placed at the center of a warm bore superconducting magnet that can reach fields of 6 T (from Ref. 48).

trap center where fortunately the trap's electric fields approach zero and are not a problem. There remains, however, a strong magnetic field. The $^9Be^+$ ion has a $2s^2S_{\frac{1}{2}}$ ground state hyperfine transition at 303 MHz which, to first order, is independent of magnetic field when $\mathbf{B} = 0.8194$ T (see Fig. 5). It is used as the clock transition.

To access this transition the trapped $^9Be^+$ ions are optically pumped into the $2s^2S_{\frac{1}{2}}(m_I = \frac{3}{2}, m_J = \frac{1}{2})$ with 313 nm radiation slightly detuned from the transition between this state and the $2p^2P_{\frac{3}{2}}(\frac{3}{2},\frac{3}{2})$ state. The slight detuning is necessary for laser cooling. While the ions cycle between these two states the fluorescence is monitored with the photon imager. The photon count rate is then a measure of the ion population in the $2s^2S_{\frac{1}{2}}(\frac{3}{2},\frac{1}{2})$ state. After about 10 s equilibrium is reached and the majority of the ions reside in the $2s^2S_{\frac{1}{2}}(\frac{3}{2},\frac{1}{2})$ state due to the optical pumping effects[36]. The 313 nm radiation is then blocked and two π-pulses are applied to transfer the ions first into the $(\frac{1}{2},\frac{1}{2})$ hyperfine state with a 321 MHz drive and then into the $(-\frac{1}{2},\frac{1}{2})$ state with a 311 MHz drive.

The field independent $(-\frac{1}{2},\frac{1}{2})$ to $(-\frac{3}{2},\frac{1}{2})$ clock transition is then interrogated using the Ramsey method of separated oscillatory fields involving two 303 MHz $\frac{\pi}{2}$-pulses which are separated in time by about 100 s. The ions remaining in the $(-\frac{1}{2},\frac{1}{2})$ state are then driven back into the $(\frac{3}{2},\frac{1}{2})$ state by reversing the previous two π-pulses. Finally, the 313 nm radiation is unblocked and the relative decrease in the fluorescence count rate represents a measure of the ion population that was transferred into the $(-\frac{3}{2},\frac{1}{2})$ state by the Ramsey interrogation of the clock transition.

This type of measurement is then taken with the frequency of the Ramsey drive alternately set to the half minimum points on opposite sides of the resonant frequency. The difference between alternating measurements is then used as an error signal to lock the average frequency of the drive to this laser cooled atomic clock. Measured stabilities of this $^9Be^+$ clock have reached about 10^{-14} and extension to the second order Doppler shift uncertainty of about 10^{-15} appears feasible.

This basic clock experiment, at various stages in its development, has been used to test fundamental aspects of physics. One of the first was a test[37] of local Lorentz invariance. This was accomplished by comparing the $^9Be^+$ clock, whose nuclear and electronic spin states are oriented with respect to the trap's magnetic field, with a hydrogen maser, whose nuclear and electronic spin states have no orientation on average because of the low magnetic field. Any coupling of the spin to a preferred direction or moving reference frame would then show up as a relative shift in the two clock frequencies as the earth rotates,

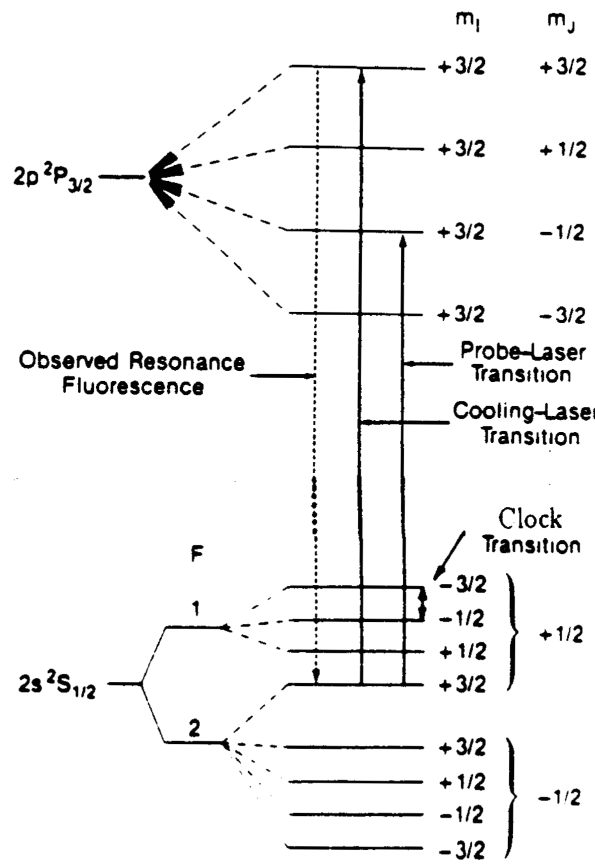

Figure 5: Hyperfine structure of $^9Be^+$ in a magnetic field, showing the transitions pertinent to the analysis of the experiments. Only the $2p^2P_{3/2}, m_I = +3/2$ states are shown because the frequency splittings between the $2p^2P_{3/2}, |\Delta m_I| = 1, |\Delta m_J| = 0$ states are on the order of 1 MHz and are therefore below the laser linewidth (from Ref. 46).

thereby changing the $^9Be^+$ clock orientation.

Along these same lines, a second set of experiments were completed which tested for unknown long range "fifth" forces that couple to spin.[38] In one the $^9Be^+$ clock frequency was compared in an experiment with the magnetic field of the trap first aligned with the earth's gravitational field and then aligned against the earth's field to look for a $\vec{\sigma}(Be)\cdot\hat{r}$ interaction where $\hat{r}$ is the direction towards a nearby large mass. No shift in the clock frequency was observed. In a similar experiment the $^9Be^+$ clock frequency was measured when the trap's magnetic field was due to a superconducting magnet, and compared with $^9Be^+$ clock frequency when the trap's magnetic field was primarily due to the polarized electrons in the pole faces of a conventional electromagnet. This looks for an unknown long range spin-spin interaction that would shift the latter clock frequency. Again no shift in the clock frequency was observed.

This clock experiment has also been used to observe a subtlety of standard quantum mechanics named the quantum Zeno effect[39] and to look for nonlinear extensions of standard quantum mechanics. The quantum Zeno effect is the inhibition of a transition between quantum states by frequent measurements of the state. Basically, the measurement process can be interpreted as projecting out a state. Time evolution of this state brings in admixtures of the second state. If a second measurement is made in a very short time after the first measurement, there will be little admixture and the most probable projection will be back into the original state. If the time evolution is quadratic for short times and the time between successive measurements is short enough, the original state will not change. The experiment[40] designed to observe this phenomenon (in the case of a stimulated transition) is a simplified version of the clock in which only the first π-pulse is applied to drive the $2s^2S_{\frac{1}{2}}(\frac{3}{2},\frac{1}{2})$ state to the $(\frac{1}{2},\frac{1}{2})$. During this π-pulse n measurements of the population of the $2s^2S_{\frac{1}{2}}(\frac{3}{2},\frac{1}{2})$ state are in principle made by briefly unblocking the 313 nm radiation. As the number of measurements increases the time between successive measurements decreases, and as predicted by the quantum Zeno effect, the population of ions transferred out of the $2s^2S_{\frac{1}{2}}(\frac{3}{2},\frac{1}{2})$ state decreases toward zero.

Recently Weinberg proposed a formalism for introducing specific nonlinearities[41] into standard quantum mechanics by modifying the Schroedinger equation to

$$i\hbar\frac{d\psi_k}{dt} = \frac{\partial h(\psi,\psi^*)}{\partial \psi_k^*}, \qquad (12)$$

where the simplest bilinear case, $h_0(\psi,\psi^*) = \psi\bar{H}\psi^*$, reduces to standard quantum mechanics. To keep the theory consistent with known experiments, homogeneity and Galilean invariance are imposed. With this modified Schroedinger equation and a nontrivial nonlinear Hamiltonian, the time evolution of a mixed state vector becomes a function of the particular admixture of eigenstates.

To test[42] for possible nonlinearities, the $^9Be^+$ clock frequency is measured with an asymmetry introduced into the Ramsey interrogation. In one run the first $\frac{\pi}{2}$-pulse is reduced to prepare the admixed state $[(1-a)^{\frac{1}{2}}(-\frac{1}{2},\frac{1}{2}) + a^{\frac{1}{2}}(-\frac{3}{2},\frac{1}{2})$ where $a < 1/2$. The frequency of this run is compared against that of a second run in which the first $\frac{\pi}{2}$-pulse is increased to prepare an admixture of states in which $a > 1/2$. In Ramsey's method of separated oscillator fields the transition frequency is defined primarily by the time evolution of the admixture of states during the time of free precession between the two $\frac{\pi}{2}$-pulses. Weinberg's theory would then manifest itself as a frequency difference between the two runs. No shift was seen which set a fractional upper limit of less than 4×10^{-27} on the nonlinear contribution to the binding energy per nucleon in the ^9Be nucleus.

NONNEUTRAL PLASMAS

In addition to reducing velocity dependent systematics errors, the low temperatures achieved through laser cooling also set up long range correlations within the "cloud" of trapped ions. There are therefore many interesting studies that can be done in the field of nonneutral plasmas.

A cloud of ions in a Penning trap has thermodynamic properties that are related to those of a one-component plasma,[43] which consists of a single species of charge embedded in a uniform neutralizing background. Here the trapping fields play the role of the neutralizing background, and laser cooling is used to manipulate the density and temperature of the plasma. Studies[44-49] that have been done so far involve looking for spatial correlations of the $^9Be^+$ ions indicative of liquid behavior and solid like crystallization that occurs when the electrostatic energy of the ion cloud dominates over the thermal energy; measuring the diffusion properties of ions within this correlated cloud; identification of collective behavior known as plasma modes (oscillations); and accessing the full range of allowed ion densities including the maximum density at the Brillouin limit.

In these studies fluorescence from the beryllium ions is imaged, as in the clock experiment, giving a time averaged two dimensional picture of the ions where the laser cooling beams intersect the cloud. This records the spatial correlations. The temperature of the cloud is determined by measuring the Doppler width of the $2s^2S_{\frac{1}{2}}(\frac{3}{2},\frac{1}{2})$ to $2p^2P_{\frac{3}{2}}(\frac{3}{2},-\frac{1}{2})$ transition with an independent "probe" laser. On resonance this probe laser takes some ions out of the $2s^2S_{\frac{1}{2}}(\frac{3}{2},\frac{1}{2})$ state and deposits them into the $2s^2S_{\frac{1}{2}}m_J = -\frac{1}{2}$ manifold through decay from the $2p^2P_{\frac{3}{2}}(\frac{3}{2},-\frac{1}{2})$ state. This tags those ions because they no longer fluoresce in the cooling beams. These tagged ions can then be used to study diffusion. Motional sidebands and Doppler shifted resonances are used to measure the rotation frequency of the cloud which can be used to calculate ion densities. Finally, the plasma modes are observed when heating occurs due to energy absorbed from resonant drives.

CONCLUSION

I have briefly described how two basic types of Penning trap experiments have found their way into various branches of physics. These include measurements of fundamental constants, precise tests of fundamental physical laws, and applied physics. To truly appreciate any of these studies, the reader is encouraged to seek out the original work referenced within.

ACKNOWLEDGMENT

I acknowledge J.C. Berquist, J.J. Bollinger, H.G. Dehmelt, G. Gabrielse, W.M. Itano, P.B. Schwinberg, R.S. Van Dyck, and D.J. Wineland as the key investigators in the Penning trap experiments mentioned above. I also thank J. Burkholder, D. Heinzen, M. Raizen, D. Sullivan, C. Weimer and M. Young for their comments on this manuscript.

REFERENCES

1. The name "geonium atom" and its implication are due to H.G. Dehmelt.
2. E.A. Cornell, R.M. Weisskoff, K.R. Boyce, R.W. Flanagan, Jr., G.P. Lafyatis, and D.E. Pritchard, "Single-Ion Cyclotron Resonance Measurments of $M(CO^+)/M(N_2^+)$," Phys. Rev. Lett. **63**,1674 (1989).
3. T.H. Malmberg, "Experiments with Pure Electron Plasmas," in *Non-Neutral Plasma Physics*, ed. C.W. Roberson and C.F. Driscoll, API Conference Proceedings **175** (American Institute of Physics, New York, 1988) p. 28.
4. G. Werth, "Precision Microwave Spectroscopy on Trapped Ions," Physica Scripta **T22**, 194 (1988), see also Ch. Gerz, D. Wilsdorf and G. Werth, "A High Precision Penning Trap Mass Spectrometer," to be published in Nuc. Instrum. Meth.
5. F. Kern, P. Egelhof, T. Hilberath, H. Kalinowski, H.J. Kluge, K. Kunz, L. Schweikhard, H. Stolzenberg, R.B. Moore, G. Audi, G. Bollen, and ISOLDE Collaboration, "Mass Measurments of Short-Lived Isotopes in a Penning Trap," in *Nuclei Far From Stability, Fifth International Conference*, ed. I.S. Towner, AIP Conference Proceeding **164** (American Institute of Physics, New York, 1988) p. 22.
6. J.Byrne, P.G. Dawber, J.A. Spain, A.P. Williams, M.S. Dewey, D.M. Gilliam, G.L. Greene, G.P. Lamaze, R.D. Scott, J. Pauwels, R. Eykens and A. Lamberty, "Measurement of the Neutron Lifetime by Counting Trapped Protons," Phys. Rev. Lett. **65**, 289 (1990)
7. G. Gabrielse, L. Haarsma, and S.L. Rolston, Int. J. Mass Spectrom. Ion Processes **88**, 319 (1989).
8. E.C. Beaty, J. Appl. Phys. **61** (6), 2118 (1987)
9. P.B. Schwinberg, R.S. Van Dyck, Jr., and H.G. Dehmelt, Bull. Am. Phys. Soc. **24**, 1202 (1979); see also R.S. Van Dyck, Jr., F.L. Moore, D.L. Farnham, and P.B. Schwinberg, Rev. Sci. Instrum. **57**, 593 (1986).
10. L.S. Brown and G. Gabrielse, Phys. Rev. **A 25**, 2423 (1982).
11. D.J. Wineland and H.G. Dehmelt, Bull. Am. Phys. Soc. **20**, 637 (1975), see also T. W. Hansch and A.L. Schawlow, Opt. Commun. **13**, 68 (1975)
12. W. Paul, O. Osberghaus, and E. Fisher, Forchungsber. Wirtsch. Verkehrsministeriums Nordhein-Westfalen No. 415 (1958).
13. A. Ashkin and J.P. Gordon, Opt. Lett. **4** 161 (1979), see also V.S. Letokhov, V.G. Minogin, and B.D. Pavlik, Zh. Eksp. Teor. Fiz. **72**, 1328 (1977).
14. R.S. Van Dyck, Jr., P.B. Schwinberg, and H.G. Dehmelt, in *New Frontiers in High Energy Physics*, Plenum, N.Y., 1978, p. 159.
15. P.B. Schwinberg, R.S. Van Dyck, Jr., and H.G. Dehmelt, Phys. Lett. **81A**, 119 (1981).
16. R.S. Van Dyck, Jr.,"Quantum Electrodynamics" Advanced Series on Directions in High Energy Physics, Vol 7, T. Kinoshita, ed. (World Scientific, Singapore,1990), pp 322-388.
17. L.S. Brown and G. Gabrielse, Rev. Mod. Phys. **58**, 233 (1986).
18. R.S. Van Dyck, Jr., P.B. Schwinberg, and H.G. Dehmelt. Phys. Rev. D **34**, 722 (1986).

19. H.G. Dehmelt, P. Ekstrom, Bull. Am. Phys. Soc. **18**, 727 (1973).

20. R.S. Van Dyck, Jr., P.B. Schwinberg, and H.G. Dehmelt, Phys. Rev. Lett. **59**, 26 (1987).

21. M.E. Cage, etal., "NBS Determination of the Fine-Structure Constant, and of the Quantized Hall Resistance and Josephson Frequency to Voltage Quotient in SI Units," in *CPEM '88 Digest*, edited by Y. Suematsu (IEEE, New York 1988), p. 333.

22. H. Dehmelt, R. Van Dyck, and P. Schwinberg, "Proposal For Detection of Geonium Spectra via Radial Displacment," Bull. Am. Phys. Soc. **24**, 491 (1979).

23. D.J. Heinzen and D.J. Wineland, Phys. Rev. A **42**, 2977 (1990).

24. R.S. Van Dyck, Jr., P.B. Schwinberg, and S.H. Bailey, "High Resolution Penning Trap as a Precision Mass-Ratio Spectrometer," in *Atomic Masses and Fundamental Constants 6*, ed. J.A. Nolen, Jr. and W. Benenson (Plenum, New York, 1980), p. 173; See also R.S. Van Dyck, Jr., F.L. Moore, D.L. Farnham, and P.B. Schwinberg, Inter. J. Mass Spectrom. and Ion Proc. **66**, 327 (1985) and Bull. Am. Phys. Soc. **31**, 244 (1986).

25. G. Gabrielse, X. Fei, L.A. Orozco, R.L. Tjoelker, J. Hass, H. Kalinowsky, T.A. Trainor, and W. Kells, Phys. Rev. Lett. **65**, 1317(1990).

26. F.L. Moore, D.L. Farnham, P.B. Schwinberg, and R.S. Van Dyck, Jr., Nuc. Instrum. Meth. Phys. Res. **B43**, 425 (1989).

27. R.S. Van Dyck, Jr., F.L. Moore, D.L. Farnham, and P.B. Schwinberg, "Mass Ratio Spectroscopy and the Proton's Atomic Mass," in *Frequency Standards and Metrology*, ed. by A. De Marchi (Springer-Verlag, Berlin, 1989) p. 349.

28. F.L. Moore, D.L. Farnham, P.B. Schwinberg, and R.S. Van Dyck, Jr., Physica Scripta **T22**, 294 (1988).

29. G.L. Green, E.G. Kessler, Jr., R.D. Deslattes, and H. Borner,Phys. Rev. Lett. **56**, 819 (1986).

30. J.J. Simpson, W.R. Dixon and R.S. Storey, Phys. Rev. C **31** 1891 (1985), see also R.G.H. Robertson and D.A. Knapp, Ann. Rev. Nucl. Part. Sci. **38**, 185 (1988).

31. R.S. Van Dyck, D.L. Farnham, F.L. Moore, and P.B. Schwinberg, from Abstracts of *12th International Conference on Atomic Physics*, Ann Arbor, Michigan ,USA, ed. W.E. Baylis, G.W.F. Drake, and J.W. McConkey (Dept. of Phys., University of Windsor, Windsor, Ontario, Canada N9B3P4 1990) II-7.

32. G.L. Greene etal, private communication.

33. A.E. Kaplan, Opt. Lett. **12**(7), 489 (1987). see also Carl S. Weimer, F.L. Moore, and D.J. Wineland, from Abstracts of *12th International Conference on Atomic Physics*, Ann Arbor, Michigan ,USA, ed. W.E. Baylis, G.W.F. Drake, and J.W. McConkey (Dept. of Phys., University of Windsor, Windsor, Ontario, Canada N9B3P4 1990) IV-15.

34. D.J. Wineland, J. Appl. Phys. **50**(4), 22528 (1979).

35. J.J. Bollinger, J.D. Prestage, Wayne M. Itano, and D.J. Wineland, Phys. Rev. Lett. **54**, 1000 (1985), see also J.J. Bollinger, S.L. Gilbert, Wayne M. Itano, and D.J. Wineland, from Proc. *4th Symposium on Freq. Standards and Metrology*, Ancona, Italy (1988) ed. A. De Marchi, (Springer Verlag, Heidelberg), p. 319.

36. Wayne M. Itano and D.J. Wineland, Phys. Rev. A 24, 1364,(1981); see also D.J. Wineland, J.C. Bergquist, Wayne M. Itano, and R.E. Drullinger, Opt. Lett. **5**, 245 (1980).

37. J.D. Prestage, J.J. Bollinger, Wayne M. Itano, and D.J. Wineland, Phys. Rev. Lett. **54**, 2387 (1985).

38. J.J. Bollinger, D.J. Heinzen, Wayne M. Itano, S.L. Gilbert and D.J. Wineland, from Proc. *12th International Conferency on General Relativity and Gravitation*, International Society on General Relativity and Gravitation (University of Colorado, Boulder, Colorado, USA, 1989), p. 500

39. B. Misra and E.C.G. Sudarshan, J. Math. Phys. **18**, 756 (1977).

40. Wayne M. Itano, D.J. Heinzen, J.J. Bollinger, and D.J. Wineland, Phys. Rev. A **41**, 2295 (1990).

41. S. Weinberg, Phys. Rev. Lett. **62**, 485 (1989). See also S. Weinberg, Ann. Phys. (N.Y.) **194**, 336 (1989).

42. J.J Bollinger, D.J. Heinzen, Wayne M. Itano, S.L. Gilbert, and D.J. Wineland, Phys. Rev. Lett. **63**, 1031 (1989), see also J.J. Bollinger. D.J. Heinzen, Wayne M. Itano, S.L. Gilbert, and D.J. Wineland, form Proc. *12th International Conference on Atomic Physics*, ed. R. Lewis and J. Zorn, (in press AIP New York).

43. J.H. Malmberg and T.M. O'Neil, Phys. Rev. Lett. **39**, 1333 (1977).

44. J.J. Bollinger and D.J. Wineland, Phys. Rev. Lett. **53**, 348 (1984).

45. D.J. Larson, J.C. Bergquist, J.J. Bollinger, Wayne M. Itano, and D.J. Wineland, Phys. Rev. Lett. **57**, 70 (1986).

46. L.R. Brewer, J.D. Prestage, J.J. Bollinger, Wayne M. Itano, D.J. Larson and D.J. Wineland, Phys. Rev. A **38**, 859 (1988).

47. Wayne M. Itano, L.R. Brewer, D.J Larson, and D.J. Wineland, Phys. Rev. A **38**, 5698 (1988).

48. S.L. Gilbert, J.J. Bollinger, and D.J. Wineland, Phys. Rev. Lett. **60**, 2022 (1988).

49. D.J. Heinzen, J.J. Bollinger, F.L. Moore, Wayne M. Itano and D.J. Wineland, submitted to Phys. Rev. Lett.